

Tracing the two- to three-dimensional transition in the InAs/GaAs(001) heteroepitaxial growth

F. Patella,* S. Nufri, F. Arciprete, M. Fanfoni, E. Placidi, A. Sgarlata, and A. Balzarotti
*Dipartimento di Fisica, Università di Roma "Tor Vergata," and Istituto Nazionale per la Fisica della Materia,
 Via della Ricerca Scientifica 1, 00133 Roma, Italy*

(Received 15 November 2002; revised manuscript received 13 February 2003; published 12 May 2003)

We have investigated by atomic force microscopy and scanning tunneling microscopy subsequent stages of the heteroepitaxy of InAs on GaAs(001) from the initial formation of the strained two-dimensional wetting layer up to the development of three-dimensional quantum dots. We provide evidence of structural features that play a crucial role in the two- to three-dimensional transition and discuss their contribution to the final morphology of the self-assembled nanoparticles. A model is suggested for the strained phase at the critical thickness consisting of an intermixed $\text{In}_x\text{Ga}_{1-x}\text{As}$ surface layer of composition $x=0.82$ and InAs "floating" on top. Such "floating" phase participate to the large mass transport along the surface during the two- to three-dimensional transition that accounts quantitatively for the total volume of dots.

DOI: 10.1103/PhysRevB.67.205308

PACS number(s): 73.21.La, 68.55.Ac, 87.64.Dz

In the lattice-mismatched heteroepitaxy of InAs on GaAs(001), depositions larger than 1.5 ML of InAs produce spontaneous self-assembling of nanoscale islands termed quantum dots (QD's). Because of the lower surface energy, the InAs initially wets the GaAs substrate; on increasing the deposited volume, the accumulated elastic strain energy is partially released by the formation of coherent 3D islands.

Albeit the details of the mechanism through which the two-dimensional (2D) to three-dimensional (3D) transition occurs are poorly understood, relatively few works have addressed this topic. There is increasing experimental evidence that the microscopic processes occurring at the early stage of the growth of the pseudomorphic interface, before 3D nucleation sets in, largely affect the final morphology of the QD arrays. Moreover, the number density, composition, single-dot volume, and total volume of the self-assembled dots differ substantially on changing single kinetic or thermodynamic parameters of the growth.

In a previous work¹ we compared dot distributions obtained by the standard continuous deposition process with those obtained by operating periodic flux interruptions during growth. Although all thermodynamic growth parameters were the same, marked differences were found in the dot volume because of the unlike involvement of the wetting layer (WL) and/or substrate in the 2D-3D transition. This result points to the relevance of kinetic limitations to the thermodynamic processes taking place in the nonequilibrium molecular beam epitaxial (MBE) growth. At the same time it suggests the importance of exploring the 2D strained phase in order to identify structural features and mechanisms being active in the 2D-3D transition.

With this aim we trace in this study the morphology of the InAs/GaAs(001) heterostructure from the initial formation of the WL up to the full development of 3D QD's, by means of scanning tunneling microscopy (STM) and atomic force microscopy (AFM). We evidence how microscopic- and mesoscopic-scale structural features, intermixing, and segregation of cations, and strain of the 2D WL determine lateral ordering, size distribution and composition of the QD's. The height and basal-area distribution of dots are determined in the growth region preceding the completion of the 3D nucleation at ~ 2 ML, where statistics can supply information on

the energetic and kinetics of the processes. We provide evidence of the intermixing of the 2D strained phase and of the presence of approximately 0.5–0.6 ML of InAs floating on top, which takes part by surface mass transport to the 2D-3D transition process.

The samples under investigation have been grown by conventional solid source MBE equipped with the reflection high-energy electron diffraction (RHEED) for *in situ* monitoring of the growth. Prior to InAs deposition, a GaAs regrowth of approximately 0.75 μm was performed on the (001) oriented substrate, in As_4 overflow, at 590 °C and at a rate of $\sim 1 \mu\text{m/h}$. After 10 min post-growth annealing, the temperature was lowered to 500 °C for the InAs deposition. This determined the transition of the GaAs(001) surface reconstruction from (2×4) to $c(4 \times 4)$. Different thickness ranging from 0.7 to 1.9 monolayers (ML), have been evaporated at a rate of 0.028 ML/s. The In delivery was cycled in 5 s of evaporation followed by 25 s of growth interruption until the given InAs thickness was reached. This procedure helps to equilibrate the surface at each deposition step by enhancing the migration of cation adatoms prior to incorporation into the lattice.² Together with low growth rate it allows us to reduce kinetic factors hindering thermodynamic driving forces.

The 2D-3D transition was recognized by the change of the RHEED pattern, along the $[110]$ azimuth, from streaky to spotty. The onset of the transition was established at the edge of the steep rise in the intensity of the RHEED signal. This onset was quite reproducible in the evaporation time scale and corresponded to the delivery of 1.55 ± 0.05 ML of InAs.

STM/AFM microscopy was performed *ex situ*, in ultrahigh vacuum. AFM images, acquired in the noncontact mode (needle sensor) with nonconductive Si tips, were used to visualize the large-scale morphology of both the WL and the QD's. Atomic scale details of the WL were revealed by STM. In this case, to preserve the surface during transport in air, the growth was terminated by deposition of a 1 μm As cap at -20 °C. The cap was removed in the ultrahigh-vacuum STM/AFM chamber at about 300 °C, and the surface was characterized by low-energy electron diffraction (LEED). The evolution cycle of the physisorbed As was

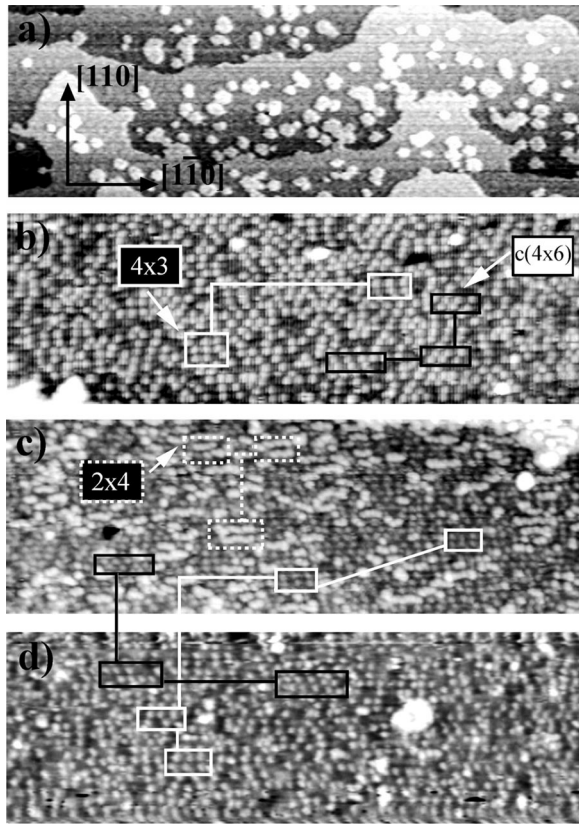


FIG. 1. (a) AFM topography, $1500 \times 500 \text{ nm}^2$, of the strained two-dimensional phase (wetting layer) obtained for 1.3 ML of InAs on GaAs (001). Atomically resolved, $30 \times 90 \text{ nm}^2$, STM images of (b) InAs wetting layer at 0.7 ML, (c) InAs wetting layer at 1.3 ML, and (d) $\text{In}_{0.2}\text{Ga}_{0.8}\text{As}$ alloy, 450 ML, grown by MBE on GaAs(001). Domains of (4×3) and $c(4 \times 6)$ periodicity are highlighted on the wetting layer and the alloy. 2×4 InAs chains are detected only on the wetting layer at 1.3 ML. The periodicity $(n \times m)$ is referred to the (001) surface cell ($a_0 \approx 4 \text{ \AA}$), n along the $[1\bar{1}0]$, and m along the $[110]$ directions.

monitored by a mass spectrometer, and care was taken not to overcome the activation temperature of the process. This procedure, commonly applied on III-V epitaxial surfaces, may introduce locally a small degree of topological disorder but maintains the original reconstruction of the underlying surface. For the strained InAs/GaAs phase, this is confirmed by comparison with published *in situ* STM data.³

The large-scale AFM topography of the WL at 1.3 ML, in Fig. 1(a), displays the typical features of the mixed-growth regime of step flow and nucleation of two-dimensional islands resulting from the combined effect of the lower surface free energy of InAs and the reduced migration length of In cations due to strain.⁴ At slightly higher InAs coverage, large 2D islands tend to coalesce giving rise to a more uniform overlayer as that shown in Fig. 2 for 1.4 ML, where, depending on the magnification of the imaged area, a different scenario is observed. At large scale, a roughened surface is revealed by the appearance of mounds of average lateral dimension $1.2 \times 0.3 \mu\text{m}^2$ and $\sim 3 \text{ nm}$ high (i.e., about ten bilayers), elongated in the $[1\bar{1}0]$ direction. Such a morphology recalls that of GaAs(001) film underneath, reproduced theo-

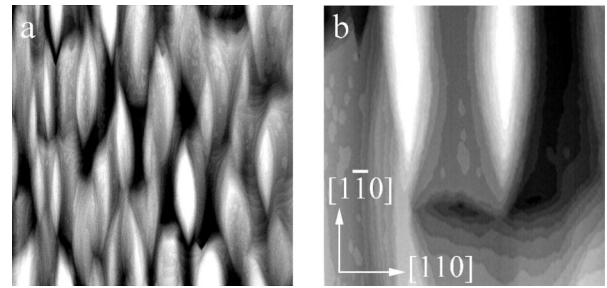


FIG. 2. (a) AFM topography, $5 \times 5 \mu\text{m}^2$, of 1.4 ML of InAs on GaAs (001). Mounds, $1.2 \mu\text{m} \times 0.3 \mu\text{m}$, about 3 nm high, are elongated in the $[1\bar{1}0]$ direction; (b) $1.5 \times 1.5 \mu\text{m}^2$ image showing terraces and meandering of steps and nucleation of 2D islands on terraces.

retically by continuum models and Monte Carlo simulations of the nonlinear late-stage regime of the homoepitaxial growth.⁵⁻⁷ The AFM topography of Fig. 2(b), reveals morphological details as step bunching, step-edge meandering, and nucleation of 2D islands on top of terraces. Growth instabilities leading to mounding of the surface can be driven energetically by a variety of kinetic mechanisms,⁸⁻¹³ which all share the common feature of breaking the symmetry between the upper and lower step edge of vicinal terraces. In many cases step bunching was attributed to the presence of impurities that pin steps.^{8,10} In a previous report¹⁴ we evidenced the striking resemblance between the large-scale morphology of the strained InAs/GaAs 2D phase, shown in Fig. 2(a), and the Monte Carlo simulation of the propagation of a 2D step-train based on the impurity model of Ref. 10. The stepped texture of the WL strongly influence the in-plane position of the 3D QD's since they nucleate preferentially at the lower edge of steps.¹⁴

To the end of understanding the 2D-3D transition it is of major relevance to establish more precisely thickness and composition of the WL, since the InAs epilayer is significantly alloyed with the GaAs substrate.³ To analyze this aspect, we report in Figs. 1(b)–1(c) the atomically resolved STM topographies of the WL at 0.7 and 1.3 ML. Notice the presence of zigzag chains on top surface plane for 1.3 ML coverage. Although the microscopy is unable to detect clearly either the intermixing of the wetting layer or its composition, the formation of an alloyed interface can be inferred by comparison with the topography of Fig. 1(d) of a strained epitaxial $\text{In}_{0.2}\text{Ga}_{0.8}\text{As}$ alloy (45 ML), grown on GaAs(001) by MBE using the same experimental procedure as for the WL. On removing the As cap, both the InAs WL and the In(Ga)As alloy surfaces displayed a dominant (1×3) LEED pattern and, only occasionally, faint traces of a (4×3) symmetry. The $\times 3$ translational symmetry of the top plane is the fingerprint for the In-Ga alloying.³ On the atomic-scale STM images of Fig. 1, small domains of (4×3) and $c(4 \times 6)$ periodicity [$4 \times$ along $[1\bar{1}0]$ and $3 \times (6 \times)$ along $[110]$ directions] are identified *both* on the wetting layer at the two different thickness and on the alloy, as marked in panels (b), (c), and (d), respectively.

More often, a “ 2×3 ” symmetry (with a weak correlation

for the $2 \times$ periodicity along the $[\bar{1}10]$ direction) is reported by *in situ* RHEED and x-ray diffraction data on InGaAs alloys¹⁵ and by *in situ* STM measurements of the 2D growth of InAs on GaAs for depositions larger than 0.8 ML.³ It should also be mentioned that a metastable “ 2×3 ” surface phase was observed on several hours annealing at 300 °C of the de-capped GaAs(001) $c(4 \times 4)$.¹⁶ However, as pointed out by Zunger *et al.*,¹⁷ the “ 2×3 ” unit cell is not charge compensated and cannot be stable. As a matter of fact, high resolution STM images¹⁶ reveal that this symmetry consists of charge compensated (4×3) and $c(4 \times 6)$ domains, similar to those we detect on the WL and on the alloy surfaces. Height profiles taken on the topography of Fig. 1 show that the $\times 3$ (and $\times 6$) translational symmetry is generally maintained over large portions of the surface, while the $4 \times$ reconstruction along $[\bar{1}\bar{1}0]$ has a correlation limited to two or three unit cells and is barely observed in LEED patterns, being the coherence area of the probe much larger than the domain sizes. One can notice that the reduced topological order, observed as well on *in situ* measurements, is also in agreement with the suggestion of Ref. 18 for the existence of a “liquid” surface layer with a certain degree of order caused by the lowering of the melting point at the high hydrostatic pressure induced by the strain.

Many experimental evidences are reported in literature on In segregation in epitaxial ternary III-V alloys leading to formation of a near-binary surface. Moison *et al.*¹⁹ estimated by x-ray photoemission and Auger measurements an average surface In composition of 0.7 for the $\text{In}_{0.2}\text{Ga}_{0.8}\text{As}$ bulk compound, grown at 480 °C. Recently it was proposed by Walther *et al.*²⁰ that the segregation of In to the surface of the initial WL in the growth of the $\text{In}_x\text{Ga}_{1-x}\text{As}/\text{GaAs}$ system (for $x \geq 0.25$) controls the critical thickness of the 2D-3D transition. Using the segregation model of Ref. 21 they derive a saturation value $x \approx 0.85$ for the surface In composition at which strain is released by islanding. By applying this model we calculated the In content of the surface and underlying layers in the cases of 45 ML of $\text{In}_{0.2}\text{Ga}_{0.8}\text{As}$, 1 and 2 ML of InAs on GaAs. On going from the top surface toward the bulk, the following values are obtained for the consecutive layers involved in the segregation process: 0.83 for the top layer of the alloy, 0.82 and 0.18 for 1 ML of InAs, and 0.99, 0.83, and 0.18 for 2 ML. We remark that the same In fraction, close to the critical value 0.85,²⁰ is predicted in the former two cases, on account of the same atomic structure detected on the surface layer of the alloy, on the subsurface of the WL at 1.3 ML and on the surface domains at 0.7 ML coverage.

An important difference exists between the alloy and the WL above 1 ML, i.e., the presence on the latter of zigzag chains, one atomic plane ($a/4 \sim 0.14$ nm) above the subsurface, having a (2×4) periodicity different from that of the substrate. One can speculate that, above 1 ML, the deposited In atoms form strained chains, that are mainly of InAs, “floating” on top of the intermixed substrate.²² This is consistent with the segregation model that anticipates a surface In fraction 0.99 on completion of the second monolayer of InAs, and with the fact that the $\text{In}_{0.82}\text{Ga}_{0.18}\text{As}$ alloyed surface

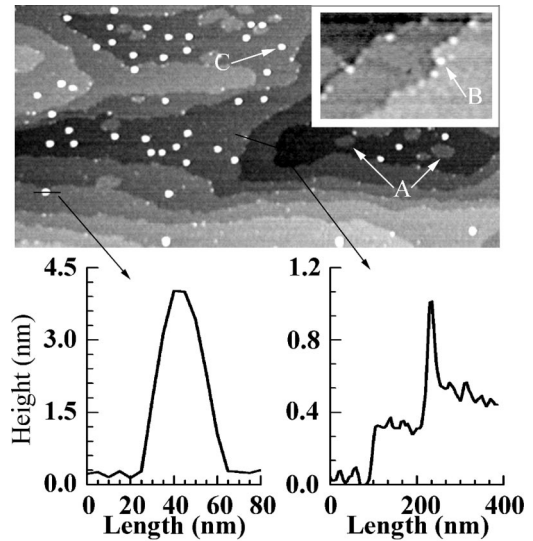


FIG. 3. AFM topography, $2 \times 1 \mu\text{m}^2$, of 1.5 ML of InAs on GaAs (001). The inset, $400 \times 250 \text{nm}^2$, evidences the nucleation of small 3D dots on the upper edge of steps. The labeled features are (a) large and small 2D-islands one monolayer high; (b) small 3D dots (quasi-3D QD) of height < 2 nm and base size ~ 20 nm; (c) 3D quantum dots (3D QD) of height 3–4 nm and base size ~ 40 nm. The height profiles of a 3D QD, and of two steps with a quasi-3D QD nucleated at the upper edge are shown.

formed on 1 ML deposition is that with the minimum Gibbs free energy.¹⁸ This model for the WL has important implications for the 2D-3D transition, at 1.5–1.6 ML, since an amount of loosely bound In, of the order 0.5–0.6 ML, is available at the surface that can participate to the surface mass transport responsible for the sudden volume increase of the 3D QDs, as will be discussed shortly.

Approaching the critical thickness (1.5–1.6 ML) the surface morphology becomes quite complex, as can be observed in the AFM images displayed in Fig. 3 for depositions ranging from 1.5 to 1.9 ML. The features to be considered for the discussion are the following: large and small 2D islands one-monolayer high, small quasi-3D islands (quasi-3D QD) of height ≤ 2 nm and base size ~ 20 nm, 3D quantum dots (3D QD's) of height 3–4 nm and base size ~ 40 nm (labeled A, B, C in Fig. 3, respectively). These features have been reported several times^{23–27} but definite conclusion on their role in QD nucleation is not yet achieved.

2D features such as those labeled A in Fig. 3 contribute only to the final morphology and to the in-plane ordering of the QD array by supplying nucleation sites.¹⁴ Conversely, features B and C (Fig. 3) require a careful consideration.

Statistical data on the quasi-3D QD and on 3D-QD's acquired in equal areas of the three samples shown in Fig. 4 are reported in the histograms inside and in Table I. We identify two clearly separated distributions for the quasi-3D QD (400–1000 atoms) and the 3D-QD (> 10000 atoms) and the gap between them do not fill in at any InAs deposition. The quasi-3D QD start nucleating between 1.4 and 1.5 ML of InAs, increase in number up to 1.7 ML and vanish above 1.9 ML, as also observed in Ref. 24. Notably, the volume of the individual dots is monotonically decreasing, while their

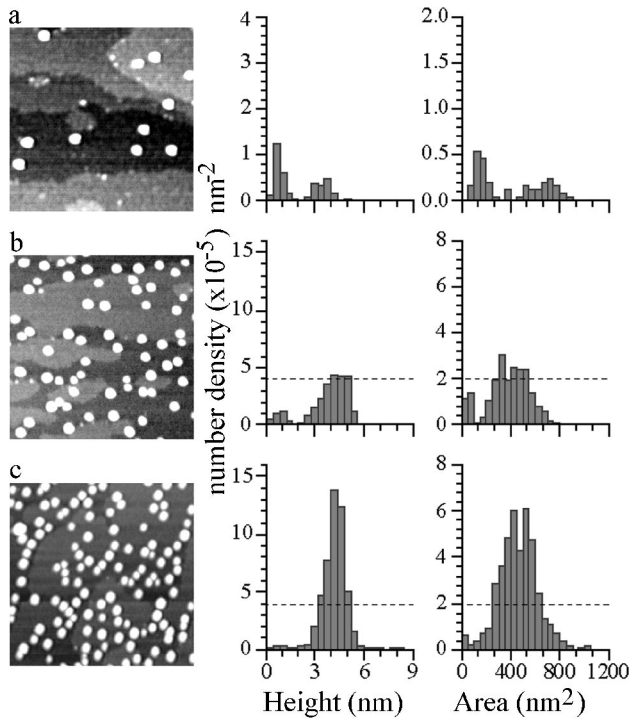


FIG. 4. AFM images $500 \times 500 \text{ nm}^2$ of InAs dots on GaAs(001) at 1.5 ML (a), 1.7 ML (b), and 1.9 ML (c). On the right side the histograms of height and basal area of quasi-3D QD and 3D QD are reported. The dashed line helps comparing low- and high-density histograms.

total volume remains negligible (see Table I). On the contrary, height and basal area distributions of the 3D-QD, between 1.5 and 1.9 ML, narrow and shift to higher and lower values, respectively, while the single-dot volume becomes stationary. These observations are consistent with the existence of two equilibrium sizes for the 3D islands, one of which (quasi-3D QD) is stable only for a limited range of InAs thickness, i.e., for a limited range of strain. The stable size of the 3D-QD has been already discussed in the literature,²⁸ and is basically related to a process of self-sizing induced by the balance between strain and bonding energy at the edge of the island. As shown in the inset of Fig. 3, small

TABLE I. Mean values of the total volume V and of the number density ρ of quasi-3D QD and 3D QD for the indicated InAs coverages Θ . The volume of the single-dot, $V_{\text{single dot}}$, is given in square brackets.

Θ	V(ML)			$\rho(10^{-4} \text{ nm}^{-2})$		
	[$V_{\text{single dot}} (\text{nm}^3)$]			quasi-3D	3D QD	total
	quasi-3D	3D QD	total	quasi-3D	3D QD	total
1.5 ML	0.008	0.067	0.075	0.22	0.15	0.37
	[130]	[1540]				
1.7 ML	0.006	0.670	0.676	0.33	2.24	2.57
	[70]	[1040]				
1.9 ML	0.0006	1.459	1.460	0.07	4.89	4.96
	[30]	[1040]				

islands have the peculiarity to nucleate at the upper-step edge of 2D islands and terraces favored by the strain relaxation and the step-down barrier for diffusing In adatoms.¹⁴ Other works also report on small 3D islands, 2–4 ML high, detected in the same²⁷ or in different^{23,29} coverage ranges, but their distribution is not reported. In Ref. 25 is found a bimodal size-distribution of 3D QD's gradually merging in a single one at increasing island density; however, this set of data is not directly comparable to the others and to ours by reason of the quite different experimental procedure used in growing the buffer layer and dots. Therefore, there is no real evidence that the nucleation of quasi-3D QD is the first step of the self-assembling process and, in this sense, quasi-3D QD's do not seem to act as precursors of 3D QD's as we have suggested¹⁴ and is stated elsewhere.²³ This consideration is supported by the evolution of the density and the volume of the 3D islands reported in Table I, which cannot be accounted for by the low density and small volume involved in nucleation of the quasi-3D QD.

At the coverage of 1.5 ML the total volume of dots is small. A large total volume variation, of about 0.6 ML, occurs at the 2D-3D transition between 1.5 and 1.7 ML (see Table I) because of the sudden nucleation of 3D QD's. At 1.9 ML the number density ρ of dots increases by a factor of 2 with respect to 1.7 ML, and by the same factor increases the total volume of 3D QD's due to the formation of equal-sized islands. These large volume variations cannot be explained only by the incoming atoms. On going from 1.5 to 1.9 ML coverage, the total volume of dots changed by 1.38 ML: a fraction of this volume 0.4 ML is due to the incoming flux while the remainder ~ 1 ML is to be accounted for by surface mass transport. If the model proposed in this work for the WL is correct, approximately 0.5–0.6 ML of “floating” In, loosely bound to the surface, will be available at the critical thickness for participating to the transition; i.e., more than 50% of that required to account for the nucleated volume of dots. Still there is an amount of missing volume, but this is consistent with the experimental evidence that self-assembled InAs/GaAs QD's are interdiffused³⁰ and participation of the substrate underneath and around islands must be invoked,¹ as occurs for other systems.³¹ More measurements are in progress to precisely quantify the contribution of the surface In and that of the substrate to the total volume of nucleated dots, and to get more insight into the 2D-3D transition mechanism.

In conclusion, by tracing the formation of 3D QD of InAs on GaAs(001) we have shown that the formation of quasi-3D QD precursors to the 3D dots is not consistent with the experimental distributions of density and volume measured in the 2D-3D transition region. It is proposed that in the heteroepitaxy of InAs on GaAs an initial intermixed $\text{In}_x\text{Ga}_{1-x}\text{As}$ ($x \sim 82\%$) layer forms on deposition of 1ML of InAs while further In deposits in form of “floating” chains on top. Such “floating” In participate to surface mass transport during the 2D-3D transition that leads to the rapid increase of the total volume of QD.

This research has been partially supported by the Ministero dell'Istruzione dell'Università e della Ricerca (Grant No. MIUR-COFIN 2000).

- *Electronic mail: patella@roma2.infn.it
- ¹F. Arciprete, F. Patella, M. Fanfoni, S. Nufri, E. Placidi, D. Schiumarini, and A. Balzarotti, in *MRS Symposia Proceedings No. 696*, edited by E.H. Chason, R. Hull, S.D. Bader, and E.A. Stach (Materials Research Society, Warrendale, 2002), p. N6.7.1; F. Patella, M. Fanfoni, F. Arciprete, S. Nufri, E. Placidi, and A. Balzarotti, *Appl. Phys. Lett.* **78**, 320 (2001).
- ²Y. Horikoshi and M. Kawashima, *J. Cryst. Growth* **95**, 17 (1989); Y. Horikoshi, in *Thin Films and Epitaxy*, Vol. 3b of *Handbook of Crystal Growth*, edited by D.T.J. Hurle (North Holland, Amsterdam, 1994), p. 691.
- ³J.G. Belk, C.F. McConville, J.L. Sudijono, T.S. Jones, and B.A. Joyce, *Surf. Sci.* **387**, 213 (1997).
- ⁴J.W. Leem, C.R. Lee, S.K. Noh, and J.S. Son, *J. Cryst. Growth* **197**, 84 (1999); T.J. Krzyzewski, P.B. Joyce, G.R. Bell, and T.S. Jones, *Surf. Sci.* **517**, 8 (2002).
- ⁵C. Orme, M.D. Johnson, J.L. Sudijono, K.T. Leung, and B.G. Orr, *Appl. Phys. Lett.* **64**, 860 (1994).
- ⁶M. Rost, P. Smilauer, and J. Krug, *Surf. Sci.* **369**, 393 (1996).
- ⁷A.L. Barabasi and H.E. Stanley, *Fractal Concepts in Surface Growth* (Cambridge University Press, Cambridge, 1995); Joachim Krug, *Adv. Phys.* **46**, 139 (1997).
- ⁸A.G. Cullis, A.J. Pidduck, and M.T. Emeny, *J. Cryst. Growth* **158**, 15 (1996); N. Cabrera and D.A. Vermilyea, *Growth and Perfection of Crystals*, edited by R. Doremus, B. Roberts, and D. Turnbull (Wiley, New York, 1958), p. 393; J.P.v.d. Eerden H. Müller-Krumbhaar, *Phys. Rev. Lett.* **57**, 2431 (1986); E.T. Croke, F. Grosse, J.J. Vajo, M.F. Gyure, M. Floyd, and D.J. Smith, *Appl. Phys. Lett.* **77**, 1310 (2000).
- ⁹R.L. Schwoebel and E.J. Shipsey, *J. Appl. Phys.* **37**, 3682 (1966); R.L. Schwoebel, *ibid.* **40**, 614 (1969).
- ¹⁰D. Kandel and J.D. Weeks, *Phys. Rev. Lett.* **72**, 1678 (1994); *Phys. Rev. B* **49**, 5554 (1994).
- ¹¹W.K. Barton, N. Cabrera, and F.C. Frank, *Proc. R. Soc. London, Ser. A* **243**, 2999 (1951).
- ¹²G.S. Bales and A. Zangwill, *Phys. Rev. B* **41**, 5500 (1990).
- ¹³P. Smilauer and D.D. Vvedensky, *Phys. Rev. B* **48**, 17 603 (1993).
- ¹⁴F. Patella, F. Arciprete, E. Placidi, S. Nufri, M. Fanfoni, A. Sgarlata, D. Schiumarini, and A. Balzarotti, *Appl. Phys. Lett.* **81**, 2270 (2002).
- ¹⁵See for instance, M. Sauvage-Simkin, Y. Garreau, R. Pinchaux, M.B. Véron, J.P. Landesman, and J. Nagle, *Phys. Rev. Lett.* **75**, 3485 (1995).
- ¹⁶I. Chizhov, G. Lee, R.F. Willis, D. Lubyshev, and D.L. Miller, *Phys. Rev. B* **56**, 1013 (1997).
- ¹⁷S.B. Zhang and A. Zunger, *Phys. Rev. B* **53**, 1343 (1996).
- ¹⁸D.J. Bottomley, *Jpn. J. Appl. Phys., Part 1* **39**, 4604 (2000), and references therein.
- ¹⁹J.M. Moison, C. Guille, F. Houzay, F. Barthe, and M. Van Rompay, *Phys. Rev. B* **40**, 6149 (1989).
- ²⁰T. Walther, A.G. Cullis, D.J. Norris, and M. Hopkinson, *Phys. Rev. Lett.* **86**, 2381 (2001); A.G. Cullis, D.J. Norris, T. Walther, M.A. Migliorato, and M. Hopkinson, *Phys. Rev. B* **66**, 081305(R) (2002).
- ²¹O. Dehaese, X. Wallart, and F. Mollot, *Appl. Phys. Lett.* **66**, 52 (1995).
- ²²J.M. Garcia, J.P. Silveira, and F. Briones, *Appl. Phys. Lett.* **77**, 409 (2000); N. Grandjean, J. Massies, and O. Tottereau, *Phys. Rev. B* **55**, R10189 (1997); R. Kaspi and K.R. Evans, *Appl. Phys. Lett.* **67**, 819 (1995); O. Brandt, K. Ploog, L. Tapfer, M. Hohenstein, R. Bierwolf, and F. Phillipp, *Phys. Rev. B* **45**, 8443 (1992).
- ²³T.J. Krzyzewski, P.B. Joyce, G.R. Bell, and T.S. Jones, *Phys. Rev. B* **66**, 121307(R) (2002).
- ²⁴T.R. Ramachandran, R. Heitz, P. Chen, and A. Madhukar, *Appl. Phys. Lett.* **70**, 640 (1997).
- ²⁵M.J. da Silva, A.A. Quivy, P.P. Gonzalez-Borrero, E. Marega, Jr., and J.R. Leite, *J. Cryst. Growth* **241**, 19 (2002).
- ²⁶N.P. Kobayashi, T.R. Ramachandran, P. Chen, and A. Madhukar, *Appl. Phys. Lett.* **68**, 3299 (1996).
- ²⁷R. Heitz, T.R. Ramachandran, A. Kalburge, Q. Xie, I. Mukhametzhano, P. Chen, and A. Madhukar, *Phys. Rev. Lett.* **78**, 4071 (1997).
- ²⁸A.L. Barabasi, *Appl. Phys. Lett.* **70**, 2565 (1997).
- ²⁹D. Leonard, K. Pond, and P.M. Petroff, *Phys. Rev. B* **50**, 11 687 (1994).
- ³⁰I. Kegel, T.H. Metzger, A. Lorke, J. Peisl, J. Stangl, G. Bauer, J.M. Garcia, and P.M. Petroff, *Phys. Rev. Lett.* **85**, 1694 (2000).
- ³¹N. Motta, F. Rosei, A. Sgarlata, G. Capellini, S. Mobilio, and F. Boscherini, *Mater. Sci. Eng., B* **88**, 264 (2002).